Conference Paper

Plasma-mediated Nanosecond-Laser Generation of Si Nanoparticles in Water

Anastasia Ivanova[1,2], Andrey Ionin[1], Sergey Kudryashov[1,2], and Irina Saraeva[1]

[1]Lebedev Physical Institute, 119991 Moscow, Russia
[2]National Research Nuclear University MEPhI (Moscow Engineering Physics Institute), Kashirskoe shosse 31, Moscow, 115409, Russia

Abstract

Plasma-mediated nanosecond IR-laser ablation of Si in water was describe sublinear function mass loss by multi shot ablative and third-power function extinction coefficient of generated colloidal solutions of density laser intensity. The first addiction shows influence subcritical ablative plasma to ablative rate, also fast increase extinction coefficient of 100 nm size particles of silicon in colloidal solution implies plasma-mediated dissociation of the ablation products.

Keywords: silicon nanoparticles, nanosecond laser ablation, sub-critical ablative plasma, extinction coefficient, scaling relationships, melt expulsion

Corresponding Author:
Anastasia Ivanova
mephynastya@gmail.com

Received: 28 January 2018
Accepted: 15 March 2018
Published: 25 April 2018

Publishing services provided by Knowledge E

Selection and Peer-review under the responsibility of the PhIO Conference Committee.

1. Introduction

Colloidal solutions of nanoparticles obtained by laser ablation are the basic form of nanomaterials, which are used in biomedicine, nanophotonics, materials science and others [1]. The high intensity of periodic pulses of the laser makes it possible to obtain ecologically and efficiently chemically pure colloidal solutions of various types of nanoparticle materials [2].

In contrast to femtosecond and picosecond laser irradiation, for which phase explosion mechanism predominates [4-6], several mechanims are well known for "dry" conditions in the nanosecond generation mode [5,7-12]. Therefore, there is a need for a proper selection of the generation parameters. As the intensity of the laser radiation increases, the following proceeds occur: 1) surface vaporization of molten materials along their "melt-vapor" binodes, ending up by short condensation of corresponding low-density atomic or small-cluster vapors [5, 13]; 2) homogeneous boiling in the proximity of their "melt-vapor" spinodes and almost coinciding with high-density facilitated optical breakdown above the ablated surface, the related onset of sub-critical plasma

How to cite this article: Anastasia Ivanova, Andrey Ionin, Sergey Kudryashov, and Irina Saraeva, (2018), "Plasma-mediated Nanosecond-Laser Generation of Si Nanoparticles in Water" in *VII International Conference on Photonics and Information Optics*, KnE Energy & Physics, pages 65–72. DOI 10.18502/ken.v3i3.2014

and ambient shock-wave emission [11]; 3) the following sub-critical plasma regulates laser energy coupling

$$\eta = 1.7 \times 10^{-6} \frac{\Psi^{9/8} I^{1/2} \tau^{3/4}}{A^{1/4} \mu \lambda^{1/2}} [\%], \tag{1}$$

surface pressurization

$$P_a = 5.83 \frac{\Psi^{9/16} I^{3/4}}{A^{1/8} \lambda^{1/4} \tau^{1/8}} [\text{dyne/cm}^2], \tag{2}$$

and ablation rate

$$\dot{m} = 2.66 \times 10^{-6} \frac{\Psi^{9/8} I^{1/2}}{A^{1/4} \lambda^{1/2} \tau^{1/4}} [\text{g/cm}^2\text{s}], \tag{3}$$

on the surface described by the well-established scaling relationships as functions of material (atomic mass A, average ion charge Z, $\Psi = 0.5A \left[Z^2 (Z+1)\right]^{-1/3}$) and laser (intensity I [W/cm^2], wavelength λ [cm] and pulsewidth τ [s]) parameters [16] and result in dissociation/ionization of ablation products in the hot plasma core above the surface prior their recombination/condensation [14-15]; 4) finally, deep material melting and superheating by transient bremsstrahlung and recombination plasma emission and its mechanical unloading during plasma adiabatic expansion [17-19] results in intense expulsion of micro-droplets [11-12,20]. Meanwhile, possible appearances of these well-known ns-laser ablation mechanims under wet ablation conditions were not firmly observed and justified yet [1, 2].

This work describes on nanosecond-laser plasma-mediated ablation of silicon wafers in water, revealing its underlying fundamental mechanisms by analyzing informative laser intensity dependences for ablative mass yield, SEM analysis and extinction coefficients of generated colloids.

2. Experimental details

For ablation was done scanning of a 0.5-mm thick, 20x20 mm^2 wide commercial monocrystalline Si under a 2-mm deionized water layer for 10 minutes by using a laser marker HTFMARK (Bulat), comprised by a Yb^{3+}-fiber laser (wavelength – 1070 nm, half-maximum pulsewidth – 120 ns, pulse energy – 1 mJ, repetition rate f_{max} = 20-80 kHz), a galvanoscanner (f ≈ 160 mm), a motorized translation from PC (Fig.1a). Laser pulses with different pulse energies E=0.4-1 mJ, coming at f = 20 kHz, were focused into a 22-μm wide (1/e-diameter $\sigma_{1/e}$) spot on a wet sample surface (Fig.1b, the peak laser fluence $F_0 \approx$ 265 J/cm^2 an the peak laser intensity $I_0 \approx$ 2.2 GW/cm^2 at E = 1mJ) and scanned across 4x4 mm^2 large area with 10-lines/mm filling at the scan velocity V = 80 mm/s.

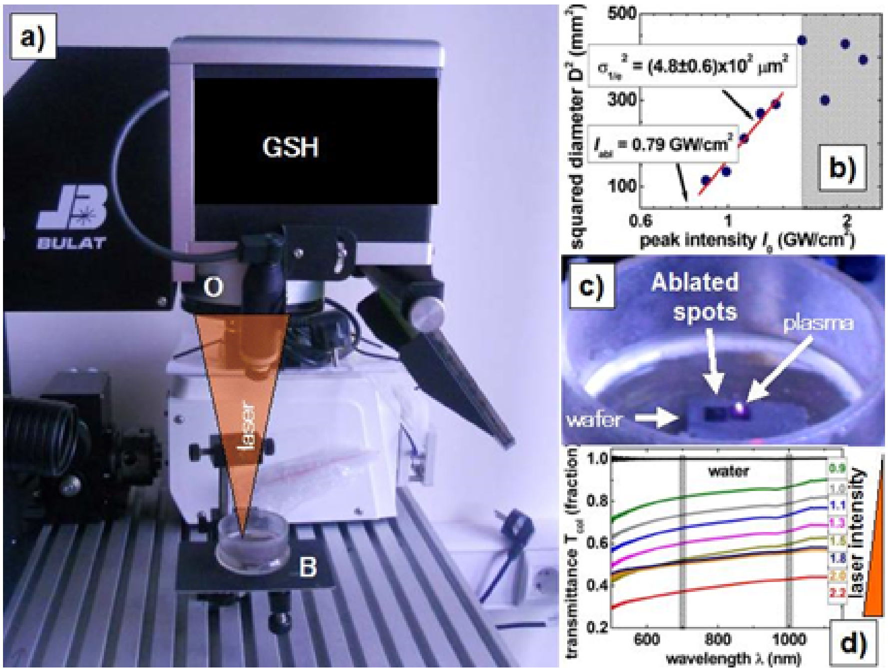

Figure 1: a) Optical image of laser ablation workstation: GSH – galvano-scanner head, O – anti-reflective objective, B – beaker with de-ionized water and silicon wafer. b) Dependence of squared ablation spot diameter, D^2, versus natural logarithm of laser intensity, $\ln I_0$, for single shot ablation with its linear fitting, providing the squared focal 1/e-diameter as the slope and the ablation threshold intensity I_{abl} as the offset. The shadowed region $I_{abl,2} \approx 1.5$ GW/cm^2 indicates the ablation instability regime related to the melt expulsion. c) Optical image of the beaker interior with the Si wafer in water and two other arrows, showing the two neighbouring ablated spots and the luminuous ablative plasma in the scanning laser beam. d) Transmittance spectra $T_{col}(\lambda)$ of silicon hydrosols at different laser intensities, shown by the correspponding color numbers in the frames on the right side.

3. Experimental results

The *single-shot* "wet" ablation spots produced at variable peak laser intensities (Fig.1b) exhibit a linear dependence in the D^2-$\ln I_0$ coordinates with the squared 1/e-diameter of the laser focal spot as the slope $\sigma_{1/e}$ = (22±1)^2 μm^2 and the *single-shot* ablation threshold I_{abl} = 0.79±0.09 GW/cm^2 as the horizontal offset. This high ablation threshold indicates the low energy coupling at the 1-μm laser wavelength to the Si sample near its indirect absoprtion edge until the material melting, yielding the strongly absorbing molten phase. The corresponding two-photon absorption (the absorption coefficient $\beta \approx 2$ cm/GW in low-intensity experiments or 50 cm/GW in high-intensity experiments), which is necessary to initiate free-carrier absorption and avalanche ionization [11], becomes considerable for the 120-ns long laser pulse only at high laser intensities, comparable to I_{abl}. At higher intensities $I_0 > I_{abl,2} \approx 1.5$ GW/cm^2 (the shadowed region in Fig.1b), the *single-shot* ablation exhibits the strong dispersion and saturation of this D^2-$\ln I_0$ curve, apparently, related to lateral plasma screening.

The obtained dependence of the sample mass loss at different intensities $I_0 > I_{abl}$ (Fig.2, left axis) demonstrates in the range I_0 = 0.9-1.5 GW/cm^2 a sublinear dependence $\Delta M_{exp} \propto I_0^{0.7\pm0.3}$, which resembles with its slope $M_L \approx 0.7$ the sub-critical plasma-mediated ablation rate dependence in Eq.(3). In contrast, a threshold-like, non-linear mass-loss increase ($\Delta M_{exp} \propto I_0^{6.7\pm0.2}$) almost by one order of magnitude occurs at higher intensities $I_0 > 1.5$ GW/cm^2 (the shadowed region in Fig.2), i.e., above the second *multi-shot* ablation threshold $I_{abl,2}$. In accordance with the previous "dry" ns-laser ablation studies, temporaly delayed expulsion of micron-sized melt droplets is expected in this second intensity range as a result of plasma-driven "bulk" phase explosion, abruptly increasing the ablation rate [12,17-20].

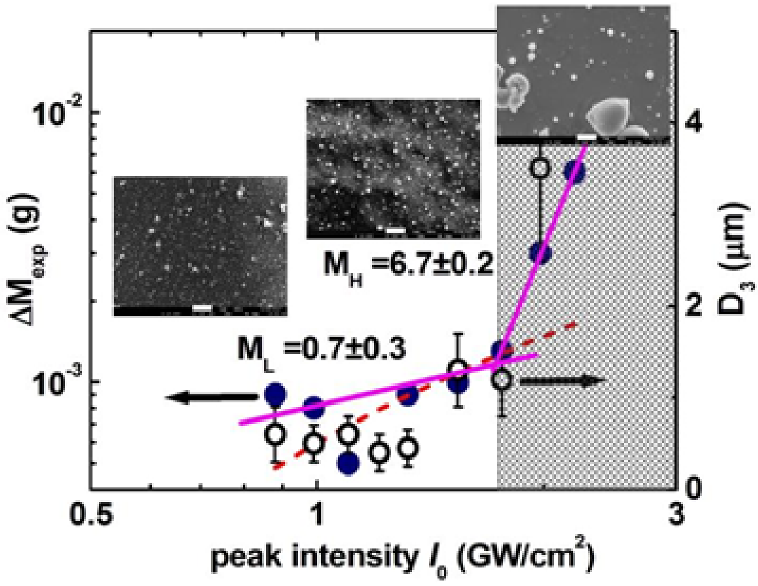

Figure 2: (left axis) Absolute mass loss ΔM_{exp} per each ablated 4×4 mm^2 spot (blue circles) versus I_0 with the shadowed high-intensity region, showing the enhanced mass removal regime for $I_0 > I_{abl,2}$, and the corresponding linear fitting curves with their slopes $M_{L,H}$. Insets: SEM images, presenting the characteristic Si nanoparticle distributions in their colloidal deposits at the corresponding intensities 1.1, 1.3 and 2.0 GW/cm^2(the scale bars are 1, 1 and 2 μm, respectively). (right axis) Average diameter of the three largest particles on each SEM image, D_3 (light circles), versus I_0.

Finally, the transmitance of the Si-NP hydrosols, rather monotonously increasing over the spectral range of 550-1150 nm (Fig.1d), was sampled in two spectral ranges – about 700 and 1000 nm – and converted to their corresponding extinction coefficients $\kappa_{700,1000}$[cm^{-1}] = ln{T_{water}(700,1000)/lnT_{col}(700,1000)} for the 1-cm long quartz cuvette (Fig.3). This quantity demonstrates for both these spectral ranges a rapid – third-power – increase above the ablation threshold I_{abl}, eventually tending to saturation for $I_0 >$ 1.5 GW/cm^2 (rather similar, threshold-like trend with non-linear arise and subsequent flattening was observed for colloidal extinction). This observation is also consistent with expulsion of micro-droplets at higher laser intensities, with such micro-droplets negligibly contributing to the colloidal extinction.

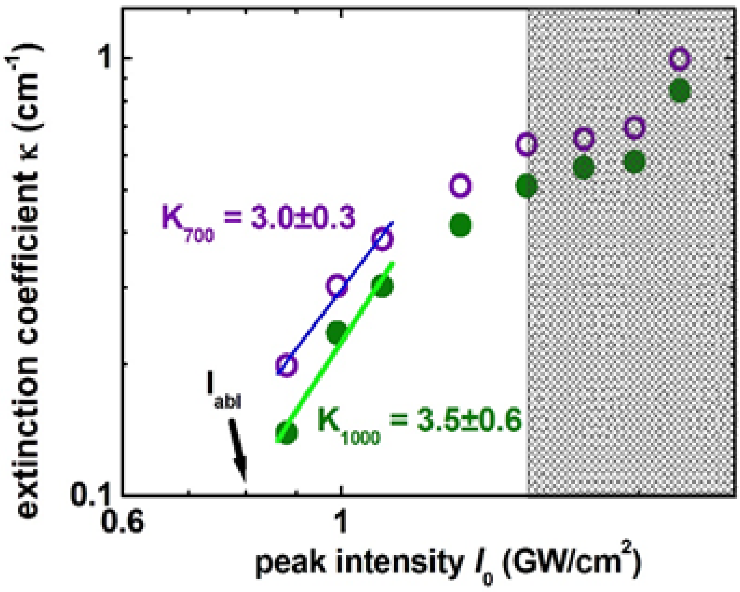

Figure 3: Extinction coefficients $\kappa_{700,1000}$ versus I_0 with the single-shot ablation threshold I_{abl} and the shadowed high-intensity region, showing the enhanced mass removal regime for $I_0 > I_{abl,2}$.

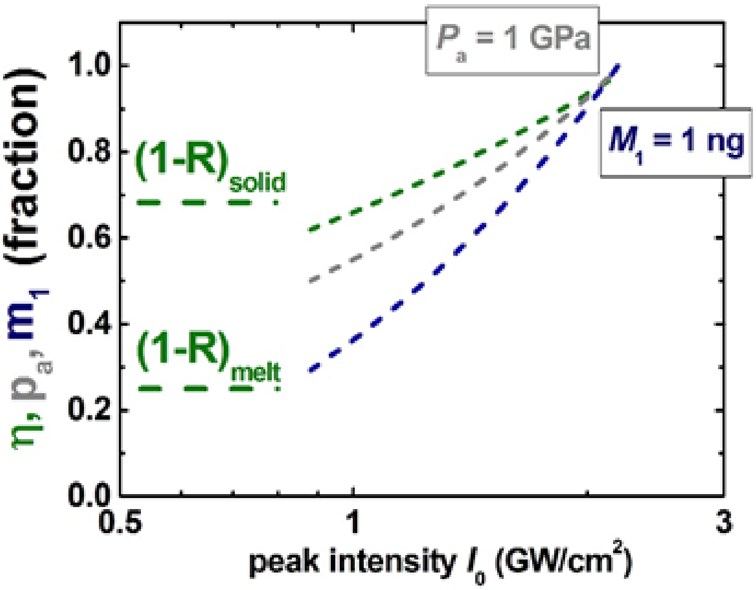

Figure 4: Intensity dependences of laser energy coupling to sub-critical plasma η, normalized plasma pressure $p_a = P/P_a$ and normalized plasma-mediated mass loss $m_1 = M/M_1$ calculated with Eqs.(1-3) for the experimental conditions of this work.

4. Conclusions

This apparently indicates that almost total redeposition can occur during the near-surface vapor buble collapse in the confined ablation regime, making nanoparticle extraction from the bubble to the ambient liquid the second important task after the ablative removal itself. Such extraction can be potentially enhanced by 1) overlapping the consequent bubbles on the surface prior collapse of the previous one and flushing (transferring) its content to the next, emerging one, being managable in the scanning regime for energy-dependent (sub)ms bubble (oscillation) lifetimes T_B and (sub)mm-wide bubble dimensions D_B [3] by changing laser repetition rate and scanning velocity to satisfy the condition D_Bf/V > 1 (apparently, this is the case in this study); 2) multi-shot repetitive ablation in the spot-by-spot ablation regime, removing by the next laser shot in each spot the material redeposited upon the previous bubble collapse; 3) multi-shot ablation at T_Bf > 1, continuously accumulating the ablated matter inside the persistent bubble.

In this study, two modes of nanosecond-laser ablation of crystalline silicon wafer in water in plasma-mediated regime were revealed by investigating mass removal and generation of corresponding colloidal solutions versus increasing laser intensity. Plasma-mediated ablation is supposed to be initiated by laser-induced "surface" phase explosion via optical breakdown of dense, hot ablative plume and results just above the ablation thresholds in characteristic sub-linear mass removal yield and third-power raise extinction of colloidal solution versus laser intensity, indicating their regulation by near-surface sub-critical plasma via surface screening and dissociation of ablation products in the hot plasma core. At higher intensities a threshold-like onset of plasma-induced bulk phase explosion is observed as a drastic raise of mass removal in the form of melt micro-droplets and the corresponding saturation of extinction dependence on laser intensity. Our findings suggest the significant role of near-surface nanosecond-laser ablative plasma in regulating primary mass and energy input, as well as driving plasma pressure inside the succeeding vapor bubble in water, which manages the accompanying nanoparticle formation/transformation dynamics.

Acknowledgments

This work was financially supported by the Russian Ministry of Science and Education (agreement no. 111111111).

References

[1] N.G. Semaltianos, ”Nanoparticles by laser ablation”, Critical Reviews in Solid State and Materials Sciences. 2010. 35. P.105.

[2] R. Streubel, S. Barcikowski, B. Gökce, ”Continuous multigram nanoparticle synthesis by high-power, high-repetition-rate ultrafast laser ablation in liquids”, Opt. Lett.. 2016. 41. P.1486.

[3] A. Letzel, B. Gökce, P. Wagener, S. Ibrahimkutty, A. Menzel, A. Plech, S. Barcikowski, ”Size Quenching during La-ser Synthesis of Colloids Happens Already in the Vapor Phase of the Cavitation Bubble”, J. Phys. Chem. C. 2017. 121. P.5356.

[4] K. Sokolowski-Tinten, J. Bialkowski, A. Cavalleri, D. von der Linde, A. Oparin, J. Meyer-ter-Vehn, S.I. Anisimov, ”Transient states of matter during short pulse laser ablation”, Physical Review Letters, 81 (1), 224-227 (1998).

[5] E. Leveugle, D.S. Ivanov, L.V. Zhigilei, ”Photomechanical spallation of molecular and metal targets: molecular dynamics study”, Applied Physics A: Materials Science & Processing, 79 (7), 1643-1655 (2004).

[6] A.A. Ionin, S.I. Kudryashov, A.A. Samokhin, ”Material surface ablation produced by ultrashort laser pulses”, Phys. Usp. 60 (2), 149-160 (2017).

[7] J.F. Ready, Effects of High Power Laser Radiation, Academic, Orlando, 1971.

[8] S.I. Anisimov, Ya.A. Imas, G.S. Romanov, Yu.V. Khodyko, Action of High-Power Laser Radiation on Metals, Nauka, Moscow, 1970.

[9] R. Kelly, A. Miotello, ”Comments on explosive mechanisms of laser sputtering”, Applied Surface Science, 96, 205-215 (1996).

[10] N.M. Bulgakova, A.V. Bulgakov, I.M. Bourakov, N.A. Bulgakova, ”Pulsed laser ablation of solids and critical phenomena”, Appl. Surf. Sci. 197, 96-99 (2002).

[11] A.A. Ionin, S.I. Kudryashov, L.V. Seleznev, ”Near-critical phase explosion promoting breakdown plasma ignition during laser ablation of graphite”, Phys. Rev. E 82, 016404 (2010).

[12] S.I. Kudryashov, A.A. Tikhov, V.D. Zvorykin, ”Near-critical nanosecond laser-induced phase explosion on graphite surface”, Appl. Phys. A 102, 493-499 (2010).

[13] G. Meijer, D.S. Bethune, ”Laser deposition of carbon clusters on surfaces: A new approach to the study of Fullerenes”, The Journal of chemical physics, 93 (11), 7800-7802 (1990).

[14] S.I. Kudryashov, S.G. Ionov, N.B. Zorov, ”Microscopic model of a charge density distribution for critical and supercritical states of carbon”, Mendeleev Communications 9 (2), 61-63 (1999).

[15] S.I. Kudryashov, ”Thermodynamic characteristics of metastable liquid-vapor equilibrium of carbon at laser vaporization of polycrystalline graphite”, PhD thesis, Moscow State University, 1999.

[16] C.R. Phipps, Jr., T.P. Turner, R.F. Harrison, G.W. York, W.Z. Osborne, G.K. Anderson, X.F. Corlis, L.C. Haynes, H.S. Steele, K.C. Spicochi, T. R. King, ”Impulse coupling to targets in vacuum by KrF, HF, and CO2 single-pulse lasers”, Journal of Applied Physics, 64 (3), 1083-1096 (1988).

[17] S. Paul, S.I. Kudryashov, K. Lyon, S.D. Allen, ”Nanosecond laser plasma assisted ultra-deep drilling of optically opaque and transparent solids”, J. Appl. Phys. 101, 043106 (2007).

[18] S.I. Kudryashov, S. Paul, K. Lyon, S.D. Allen, ”Dynamics of laser-induced surface phase explosion in silicon”, Appl. Phys. Lett. 98, 254102 (2011).

[19] N.M. Bulgakova, A.B. Evtushenko, Yu.G. Shukhov, S.I. Kudryashov, A.V. Bulgakov, ”Role of laser-induced plasma in ultradeep drilling of materials by nanosecond laser pulses”, Applied Surface Science 257, 10876-10882 (2011)

[20] J.H. Yoo, S.H. Jeong, R. Greif, R.E. Russo, ”Explosive change in crater properties during high power nanosecond laser ablation of silicon”, Journal of Applied physics, 88 (3), 1638-1649 (2000).